

# Supplemental Material for “Quantum domain walls induce incommensurate supersolid phase on the anisotropic triangular lattice”

Xue-Feng Zhang,<sup>1,2,3,\*</sup> Shi-Jie Hu,<sup>1,†</sup> Axel Pelster,<sup>1</sup> and Sebastian Eggert<sup>1</sup>

<sup>1</sup>*Physics Dept. and Res. Center OPTIMAS, Univ. of Kaiserslautern, 67663 Kaiserslautern, Germany*

<sup>2</sup>*Max-Planck-Institute for the Physics of Complex Systems, 01187 Dresden*

<sup>3</sup>*State Key Laboratory of Theoretical Physics, Institute of Theoretical Physics, Chinese Academy of Sciences, Beijing 100190, China*

(Dated: August 1, 2016)

In the Supplemental Material additional information on the performed Quantum Monte Carlo (QMC) simulations are given. Further results as a function of hopping strength and system size are shown. In addition to periodic boundary conditions, cylindrical boundary conditions also are considered. Finally, details on the derivation of the effective interaction energy between the domain walls are presented.

## I. QUANTUM MONTE CARLO METHOD

For the numerical quantum Monte Carlo (QMC) simulations we implemented the cluster stochastic series expansion method [1–3] by taking into account three sites as the update unit, as it can help increasing the ergodicity [3]. It is well known that QMC may have an infamous minus sign problem if an exchange of two fermions is possible, or if a kinetic frustration occurs, i.e. the overall probability of an off-diagonal exchange along a closed loop is negative. Since we are dealing with bosons with positive hopping our model is without sign problem, despite the triangular geometry.

However, another typical QMC problem of trapping in a local minimum is indeed of concern for our studies. In particular, the domain walls in the incommensurate supersolid phase represent very robust topological defects, so the system may get trapped at a fixed domain wall number, which is difficult to change with a small hopping parameter even using the loop update. In addition, because the wave functions with different domain wall numbers have nearly no overlap, also ordinary parallel tempering [4] does not show much improvement. In order to solve this local minimum problem, a further extension of the parallel tempering method has been developed. To this end we perform the normal QMC simulation in the whole parameter region first and store the configuration at each point. Then, for each parameter point, we use the outcome of neighboring parameter points as the initial configuration and launch additional simulations. When they are finished, we choose the simulation with the lowest average energy as the right one since at low temperatures we are effectively in the ground state limit. We find that without this change of initial configurations the resulting energy curve is discontinuous as a function of parameters, but it becomes continuous after the swap. Only for larger hopping parameters, such

as  $t/V = 0.1$ , the ordinary parallel tempering with loop update can overcome the local minimum.

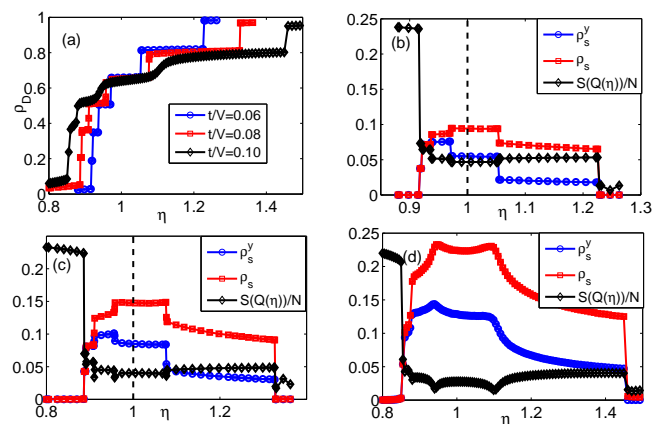


FIG. 1: (a) Bosonic domain wall density as function of anisotropy parameter  $\eta$  at  $t/V = 0.06, 0.08, 0.10$ . (b-d): Total superfluid density  $\rho_s$ , its value in  $y$ -direction  $\rho_s^y$ , and structure factor  $S(\mathbf{Q})/N$  at  $t/V = 0.06$  (b),  $t/V = 0.08$  (c),  $t/V = 0.10$  (d). All QMC results have been obtained for  $\beta V_{\max} = 200$  and  $L = 12$  with periodic boundary conditions.

## II. PHASE TRANSITIONS

The domain wall picture works well in the strong-coupling limit. In fact up to first-order perturbation theory in the hopping parameter, the ground states with different domain walls have no overlap, so there are no corrections to the quantized values of the domain wall numbers. In the following we illustrate the effect of changing hopping close to (but below) the superfluid transition at  $t'/V' \approx 0.11$  [5]. Figure 1 (a) shows that the steps are very clearly visible in the strong-coupling region at  $t'/V' = 0.06$ , but relaxation of the plateaus is observed when the hopping is increased to  $t'/V' = 0.1$ . The same is true for the step-like structure for all order parameters in Fig. 1(b-d). For larger hopping  $t'/V' = 0.1$  and near

\*Corresponding author: xuefeng@pks.mpg.de

†Corresponding author: shijiehu@physik.uni-kl.de

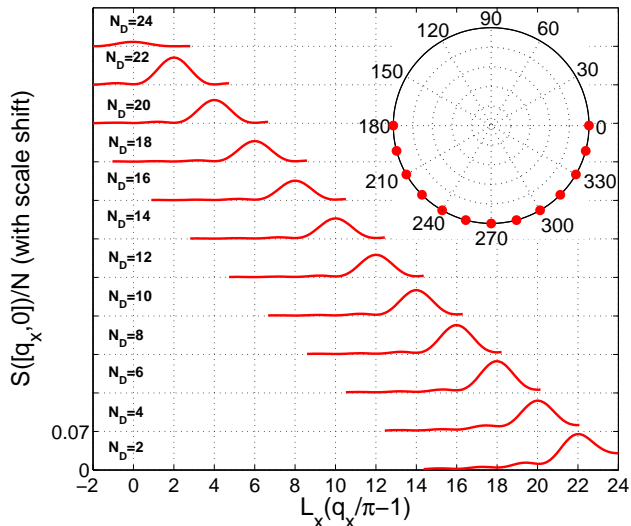


FIG. 2: Structure factor  $S(\mathbf{Q})/N$  as function of  $q_x$  at  $q_y = 0$  for different domain wall densities (shifted relative to each other) at  $t/V = 0.08$ ,  $L = 24$ , and  $\beta V_{\max} = 400$ . Inset: Maximum position (red dot) of  $S(\mathbf{Q})/N$  in  $q_x$ -direction for  $q_y = 0$  using values of  $\eta$  corresponding to different domain wall numbers  $N_D$ .

the ends of the plateaus, we observe maxima in the superfluid density and minima in the structure factor due to increased fluctuations in Fig. 1(d), but the qualitative signature of domain walls always remains visible.

One of the main results in the paper is that each plateau of the domain wall density is closely related to a corresponding maximum of the structure factor. In order to make this connection clearer, we plot the structure factor  $S(\mathbf{Q})/N$  in  $q_x$ -direction for  $q_y = 0$  using values of  $\eta$  in the center of the corresponding domain wall plateau in Fig. 2. The positions of the peaks match well with the analytic prediction  $N_D = L_x(2 - q_x/\pi)$ .

### III. FINITE-SIZE SCALING

In the paper we demonstrated that the quantization of the domain wall density becomes continuous in the thermodynamic limit. This implies that the shift of the structure factor is also continuous at the phase transition, indicating a second-order phase transition. To give additional support we present the finite-size scaling of the superfluid density difference between the two phases at  $\eta_{c1}$  in Fig. 3. Clearly, the second-order polynomial fit shows that the jump also vanishes in the thermodynamic limit for this order parameter, which confirms that the phase transition is of second order.

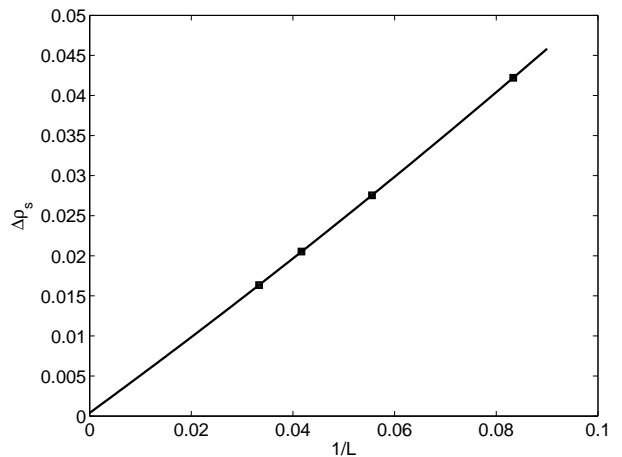


FIG. 3: Finite-size scaling of superfluid density difference between the two phases at  $\eta_{c1}$  for  $t/V = 0.08$ ,  $\beta V_{\max} = 200$ , and  $L/12$ .

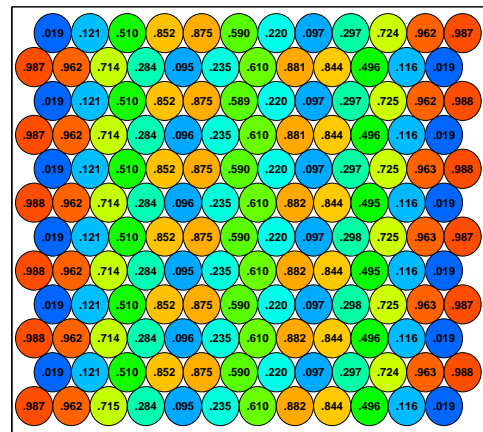


FIG. 4: Average bosonic density distribution at  $t/V = 0.08$ ,  $\beta V_{\max} = 200$ ,  $\eta = 0.9$ , and  $L = 12$  with  $y$ -cbc.

### IV. CYLINDRICAL BOUNDARY

Whereas so far we have chosen periodic boundary conditions, we investigate now cylindrical boundary conditions ( $y$ -cbc) with open ends in  $x$ -direction. In that case single domain walls can be created, so the number of domain walls  $N_D = \rho_D L$  can be both even or odd integers, which is indeed seen in the simulations. Furthermore, Fig. 4 shows that the fluctuating domain walls are clearly visible in terms of regions of average half-filling, which separate regions of checkered order, the latter being particularly stable near the edges. All these observations strongly support the quantum nature of domain walls, and rule out classical explanations of incommensurate order, such as a continuous spiral rotation of the spin [6].

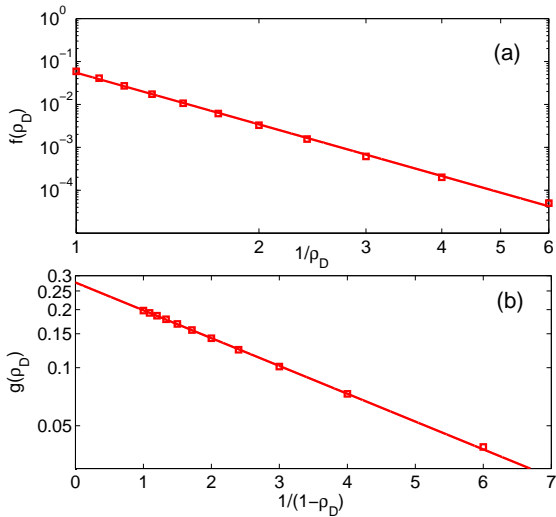


FIG. 5: Fitting of interaction energies between two neighboring (a) domain walls  $f(\rho_D)$ , (b) density pairs  $g(\rho_D)$  for  $t/V = 0.08$ ,  $\beta V_{\max} = 400$ , and  $L = 24$ .

## V. EFFECTIVE INTERACTION ENERGIES

In this section, we discuss a phenomenological model how to determine the effective interaction energies between two neighboring domain walls for  $\eta < 1$  and density pairs for  $\eta > 1$  from QMC data. At first, we discuss the dilute domain wall case  $\eta < 1$ . The total energy of  $N_D$  domain walls is given by

$$E(N_D) = N_D L_y \left[ \frac{V' - V}{2} - \frac{2}{\pi} t' / V' + f \left( \frac{N_D}{L_x} \right) V' \right], \quad (1)$$

as discussed in the Letter. Here the first term corresponds to the potential energy with  $V = \eta V'$ , the second term denotes the kinetic energy. The third term models the repulsive interaction energy between the domain walls, where the function  $f(N_D/L_x)$  takes into account the dependence on the distance  $L_x/N_D$  between two domain walls. Thus, we arrive at

$$E(N_D) = V' N_D L_y \left[ \frac{1 - \eta}{2} - \frac{2}{\pi} t' / V' + f \left( \frac{N_D}{L_x} \right) \right]. \quad (2)$$

Due to periodic boundary conditions the number of domain walls  $N_D$  changes by multiples of 2. In order to analyze the respective transitions from  $N_D = 2M - 2$  to  $N_D = 2M$  with  $M = 1, \dots, M_{\max} = L_x/2$  we have to evaluate the conditions

$$E(N_D = 2M - 2) = E(N_D = 2M). \quad (3)$$

This yields the position of the jumps between the plateaus

$$\eta_M = 1 - \frac{4}{\pi} t' / V' + 2M f \left( \frac{2M}{L_x} \right) - (2M - 2) f \left( \frac{2M - 2}{L_x} \right). \quad (4)$$

By formally identifying  $\eta_0 = \eta_{c1} = 1 - 4t'/V'\pi$ , the respective jump points with different domain wall numbers read explicitly

$$\begin{aligned} \eta_1 &= \eta_{c1} + 2f(2/L_x) \\ \eta_2 &= \eta_{c1} + 4f(4/L_x) - 2f(2/L_x) \\ \eta_3 &= \eta_{c1} + 6f(6/L_x) - 4f(4/L_x) \\ &\vdots \end{aligned} \quad (5)$$

Thus, we deduce from (6) that the effective interaction energy can be reconstructed from the values at which the jumps occur according to

$$f \left( \frac{2M}{L_x} \right) = \sum_{i=1}^M \frac{\eta_i}{2M} - \frac{\eta_0}{2}. \quad (6)$$

Using the jump points from QMC simulations (c.f. Fig. 2 in the Letter) we determine via Eq. (7) the effective interaction energy between two domain walls  $f(\rho_D)$  for a finite density  $\rho_D = N_D/L_x$ . The results are shown in Fig. 5 (a) on a double logarithmic scale and clearly indicate a simple power law

$$f(\rho_D) \sim \rho_D^\alpha, \quad (7)$$

with  $\alpha = 4 \pm 0.1$ . The same strategy turns out to be also applicable in the decoupled chain region with neighboring density pair excitations, i.e.  $1 < \eta$ . The only difference is that now  $\eta_0 = \eta_{c2}$  and the effective interaction energy between two neighboring density pairs is denoted by another function  $g(\rho_D)$  with  $g(\rho_D = 1) = 0$ . The corresponding fit in Fig. 5 (b) reveals that the effective interaction energy  $g(\rho_D)$  is given by an exponential

$$g(\rho_D) \sim \exp \left( -\frac{1}{\gamma(1 - \rho_D)} \right), \quad (8)$$

with  $\gamma = 3 \pm 0.05$ . The results in Eqs. (8) and (9) are used in the Letter to derive a relation between  $\eta$  and  $\rho_D$  in thermodynamic limit.

- 
- [1] A. W. Sandvik, Phys. Rev. B **59**, R14157 (1999);  
 [2] O. F. Syljuåsen and A. W. Sandvik, Phys. Rev. E **66**, 046701 (2002).  
 [3] K. Louis and C. Gros, Phys. Rev. B **70**, 100410(R) (2004).  
 [4] P. Sengupta, A.W. Sandvik, and D.K. Campbell Phys. Rev. B **65**, 155113 (2002).

- [5] S. Wessel and M. Troyer, Phys. Rev. Lett. **95**, 127205 (2005).  
 [6] W. Zheng, R. H. McKenzie, and R. R. P. Singh, Phys. Rev. B **59**, 14367 (1999).